RESEARCH REPORT ISIS-RR-94-14E

Graph Drawing by Magnetic-Spring Model

Kozo Sugiyama and Kazuo Misue

August, 1994

Institute for Social Information Science,
FUJITSU LABORATORIES LTD.

Nnmazu office
140 Miyamoto, Numazu, Shizuoka, 410-03, Japan
Telephone: +81-559-23-2222 Fax: +81-559-24-6180

Tokyo office
9-3 Nakase 1-chome, Mihama-ku, Chiba-shi, Chiba 261, Japan
Telephone: +81-43-299-3211 Fax: +81-43-299-3075

Graph Drawing by Magnetic-Spring Model

Kozo Sugiyama and Kazuo Misue

Institute for Social Information Science,
FUJITSU LABORATORIES LTD.
140 Miyamoto, Numazu, Shizuoka, 410-03, Japan
E-mail address: {sugi,misue}@iias.flab.fujitsu.co.jp

Abstract

A novel method for drawing graphs is proposed introducing a new model called magnetic-spring model that is an extension of Eades's spring model. Graph drawing by force-directed placement so far has been investigated mainly for undirected graphs and an idea of controlling edge orientations has not been considered. The proposed method can control edge orientations and nicely draw not only undirected graphs but also other classes of graphs such as trees, directed graphs and mixed graphs in a simple and unified manner. Moreover, since the method is conceptually intuitive, it is quite easy to understand, implement and improve it. A magnetic-spring model is defined imitating the physical system and a magnetic-spring algorithm is presented. Many layouts and results from statistical experiments are shown to demonstrate extensive effectiveness of the proposed method.

Key words: magnetic-spring model, graph, algorithm, graph drawing, visualization

1 Introduction

The problem of graph drawing concerns how to produce *nice* or *aesthetically-pleasing* pictures of graphs on a plane. A lot of methods for drawing graphs have been proposed so far according to different classes of graphs, different styles of representation, or different purposes of applications[1]. In developing methods for drawing undirected graphs, two types of approaches can be distinguished: *force-directed placement* [2,3,4] and *graph theoretic* [5,6,7]. Since the former approach is based upon the idea of simplified simulations of physical systems, it is substantially heuristic, but is conceptually intuitive and easier to be understood and implemented than the latter.

Eades[2] presented an algorithm based upon the *spring model* for drawing undirected graphs. In the model, vertices are replaced with steel *rings* and each edge with a *spring* to form a mechanical system, and repulsive and attractive forces are defined among rings. (See Figure 1a.) Then the rings are placed in some initial layout and moved iteratively according to the forces so that the system reaches a minimal energy state. Finally rings are drawn as points or small circles, and each edge as a straight line segment between a pair of rings connected by the edge. Kamada[4] proposed more sophisticated formulation and algorithm based on Eades's model, and Fruchterman & Reingold[3] presented an effective modification of the model. In these algorithms the formulae of the forces defined among rings are different from each other and they all do not reflect the natural reality directly. Aesthetic criteria generally accepted in the force-directed placement approach have been: uniforming edge lengths (A1), minimizing edge crossings (A2), revealing symmetry (A3), distributing vertices evenly (A4) and conforming to the frame (A5).

In this paper we introduce a new aesthetic criterion, conforming edges to specified orientations (A6), and propose a method based on a new model called *magnetic-spring model.* In this model, vertices are replaced with rings and edges with *magnetic springs*, and various types of magnetic fields are defined. (See Figure 1b.) With this model we can not only obtain the placement of vertices satisfying the above generally accepted aesthetic criteria, but also control the geometrical orientations of edges (or magnetic springs) by the rotative forces exerted on the edges. This can bring us novel capabilities in graph drawing by force-directed placement. Though the force-directed placement approach has been carried out mainly for drawing undirected graphs, our method is effective for drawing several types of graphs: trees, directed graphs, undirected graphs and *mixed graphs* (graphs with both directed and undirected edges). There already exist special drawing algorithms for each type of graphs. However, if people could draw nicely different types of graphs with the simple and unified method proposed in this paper, this contributes not only to the force-directed placement approach itself, but also to graph drawing in general.

Figure 2 shows examples of diagrams appeared in the literature that imply the plausibility of introducing the forces to control edge orientations in graph drawing:

1. Binary tree (Figure 2a): This is a list structure diagram drawn by a special tree drawing algorithm[8]. It is desirable to attain strictly that *car*-edges are drawn vertically and *cdr*-edges horizontally. A tree with two types of edges as a list structure is called an *edge-bipartite tree* here.
2. Directed graph (Figure 2b): This diagram expresses causal relationships and seems to be drawn manually[9]. With the automatic drawing every edge except two both-way relationships should be drawn upward and the both-way relationships horizontally.
3. Mixed graph (Figure 2c): This is an issue map in which four types of relationships are used: one is one-directional and the rest three are bi-directional [10]. How to control these four types of edges is a quite interesting problem.

Our results of drawing these examples will be shown in the third section. Besides we make many experiments to test the ability and effectiveness of our method to produce aesthetically-pleasing pictures.

In the next section our new method based upon a magnetic-spring model is described. Experimental results and discussions are shown in the third section. Finally concluding remarks are made with suggestions for future research, where envisaged are diversifying the idea of "field" and extending "virtual" models.

2 Proposed Method

In developing a new method, we adopt three principles for graph drawing: (1) vertices connected by an edge should be drawn near each other, (2) vertices should not be drawn too close to each other, and (3) each edge should be drawn according to some pre-assigned orientations as much as possible. The first two principles are just same as those of Eades[2] and Furuchterman & Reingold[3], and the last one is our new principle.

2.1 Magnetic-Spring Model

A graph $G=(V, E)$ consists of a set V of vertices and a set E of pairs of vertices. An element of E is called an edge. A graph $G=(V, E)$ is modeled as a mechanical system of rings and magnetic springs placed in a magnetic field on a plane. This model does not reflect the natural reality readily or is characterized as a "virtual" model as well as the spring model.

1. Every vertex in V is replaced with a steel *ring*. (See Figure 1.)

2. Edges in E are classified into *magnetic edges* and *non-magnetic edges.* Magnetic edges are replaced with *magnetic springs* to control orientations of the edges and non-magnetic edges simply with *springs.* Magnetic springs consist of *one-directional magnetic springs* and *bi-directional magnetic springs.* (See Figure 3.) Usually directed edges are assigned as magnetic edges and replaced with one-directional magnetic springs Undirected edges are usually assigned as non-magnetic edges but sometimes they are assigned as magnetic edges and replaced with bi-directional magnetic springs . How to assign such the magnetic property of edges substantially depends on applications.

3. We consider three types of *standard magnetic fields* : parallel, polar and concentric; and two types of *compound magnetic fields* : orthogonal and polar-concentric. Compound magnetic fields are composed from standard magnetic fields. (See Figure 4.) When we put $b(x,y)$ and $\boldsymbol{m}(x,y)$ the strength of a magnetic field and the orientation vector that expresses the orientation of the field at any point (x,y) respectively, each standard magnetic field $B(x,y)$ at (x, y) is given by

$$B(x,y) = b\,\boldsymbol{m}. \tag{1}$$

In this paper we consider uniform fields for simplicity and so we put b is constant at any point (x,y) except the origin(0, 0) and we put $\boldsymbol{m}$ as follows:

(1) parallel field :

$$\boldsymbol{m} = (0, 1) \quad \text{(north)}, \qquad (-1, 0) \quad \text{(west)}, \qquad (0, -1) \quad \text{(south) or} \qquad (1, 0) \quad \text{(east)}; \tag{2}$$

(2) polar field:

$$\boldsymbol{m} = (x, y)/|(x, y)|, \tag{3}$$

specially $B(0, 0) = 0$;

(3) concentric field:

$$\boldsymbol{m} = (y, -x)/|(x, y)| \quad \text{(clockwise) or} \tag{4}$$

$$(-y, x)/|(x, y)| \quad \text{(anti-clockwise),}$$

$$\text{specially } \boldsymbol{B}(0, 0) = 0.$$

4. We consider three types of *forces* ; F_s : attractive or repulsive forces exerted by the springs between neighbors, F_r : repulsive forces between every pair of non-neighboring vertices and F_m : rotative forces exerted on edges by the magnetic field. (See Figure 3.) The ideas of the first two forces are based on Eades's model. The last is calculated as forces exerted on the vertices connected by each magnetic edge. Strengths of these forces are given by:

$$F_s = c_s f_s(d) \tag{5}$$

$$F_r = -c_r f_r(d) \tag{6}$$

$$F_m = c_m b d^{\alpha} \theta^{\beta} \tag{7}$$

where d is the distance between a pair of vertices, $-\pi < \theta < \pi$ is the angle (radian) from the orientation of the field to the orientation of the magnetic edge, and α, β, c_s, c_r, $c_m > 0$ are parameters for tuning the model. In the case of a bi-directional magnetic edge, there can exist two angles θ_1(negative) and θ_2 (positive). We select for θ the one of which absolute value is smaller than that of the other. Though magnetic forces F_m are exerted on each magnetic edge by a magnetic field, we calculate them as two forces (with a same strength and reverse orientations) exerted on a pair of vertices connected by the edge. (See Figure 3) In Eades's model, the first two forces F_s and F_r are given as $f_s(d) = \log(d/k)$ and $f_r(d) = 1/d^2$ respectively, and in Fruchterman & Reingold's model, $f_s(d) = d^2/k$ and $f_r(d) = k$

$^2/d$ respectively where k expresses an *ideal distance* between neighbors. Which of standard magnetic fields each magnetic edge reacts selectively is pre-assigned.

5. We introduce special rings called *anchor rings* which never be moved even if some force is exerted on the rings. We can extend the idea of anchor rings to *anchor bars* and *anchor frames*, but we do not use anchor bars and anchor frames in this paper.

2.2 Algorithm

Our algorithm is based upon Eades's algorithm in which the mechanical system is simulated. Before starting calculations we should specify natures of spring and repulsive forces as F, a type of magnetic field as M and types of edges in terms of magnetic responses as R.

algorithm MAGNETIC_SPRING (G: graph, F: spring and repulsive forces,
M: magnetic field, R: specifications of magnetic responses);

1. place vertices of G on a circle evenly, of which radius is $k\,|V|/2\pi$, in a random order;
2. repeat n times
   2.1 calculate the force exerted on each vertex by composing three kinds of forces according to F, M, R;
   2.2 move each vertex by $\delta \times$ (force on the vertex);
3. draw the graph on a screen.

Parameter δ controls the magnitude of moving steps. Calculations of forces F_s's, F_r's and F_m's have $O(|E|)$, $O(|V|^2)$ and $O(|E|)$ time complexity respectively. An initial placement of vertices on a circle can be seen in Figure 6a.

3 Experimental Results

In this section, we present examples of diagrams drawn with our algorithm in order to show the usefulness of controlling edge orientations and we test the capabilities of our method by statistical experiments. In the experiments we randomly generate thirty sample graphs, all of which are connected, for various cases such as:

classes of graphs: rooted trees (RT), acyclic directed graphs (ADG), cyclic directed graphs (CDG), edge-bipartite rooted trees (EBRT) or acyclic mixed graphs (AMG);

the number of vertices: 20 or 40;

mean degree: 2.5 or 3.0 (nearly 2 in the case of trees).

Then we apply our algorithm to the sample graphs in various magnetic fields shown in Figure 4 and calculate the following five quantitative criteria:

CROSSING: the number of crossings (which relates to aesthetic criterion A2),

EDGE ORIENTATION : the distribution of angles between the orientations of edges and the given magnetic field (A6),

ERROR EDGE: the number of edges of which orientations do not conform to the magnetic field (A6),

EDGE LENGTH: the distribution of edge lengths (A1) and

VERTEX DENSITY: the density of vertices distribution (A4) measured as the mean minimum distance between a vertex and its non-neighbor vertices.

We do not consider aesthetic criterion A5 here. In the experiments default values of parameters are set as $\alpha = 1.0, \beta = 1.0, c_s = 2.0, c_r = 1.0, c_m = 1.0$ and $k = 1.0$. Parameter b is changed between 0.0 and 16.0 to observe effects due to the strength of a magnetic field. Parameter δ is changed between 0.005 and 0.1 so that the larger b is, the smaller δ is, which is to make the length of a moving step equal through simulations. Therefore the number of steps diverges from 100 to 1600. Examples of diagrams and experimental results from the magnetic-spring algorithm are shown in the following subsections.

3.1 Results in parallel field

3.1.1 Rooted trees

Both Eades[11] and Fruchterman & Reingold[3] reported the difficulty of drawing trees without edge crossings by spring algorithms. Figure 5 shows the example explaining a potential barrier for this problem (see figure 42, in [3]). However, we can overcome it and obtain a good layout of the same graph by using our magnetic-spring algorithm. Figure 6a shows an initial placement of the graph. If there does not exist any magnetic field, we obtain the layout shown in Figure 6b where we can not eliminate a crossing, whereas if there exists a strong parallel field, we obtain the crossing-free layout shown in Figure 6c. Figure 6c is laid out in a "tree" form, but the diagram is too narrow due to the existence of the strong field. Therefore, we further continue the calculation in no magnetic field as the next phase and then we get the symmetrical layout presented in Figure 6d. Thus this *two-phase* algorithm is quite effective to obtain good layouts of rooted trees.

The good performance to reduce the number of crossings in drawing rooted trees by our algorithm is also confirmed from statistical experiments. Figure 7 shows the experimental results in a parallel field where for rooted trees the expected number of crossings is very low and every edge conforms to the orientation of the field when the strength of the field is high.

3.1.2 Acyclic directed graphs

With the magnetic-spring algorithm we can realize easily downward (or upward) layouts of acyclic directed graphs. Figure 8 shows variations of layouts of an acyclic directed graph when the strength of the magnetic field is changed.

Figure 8a corresponds to the case of no magnetic field and Figure 8f the strongest. We can see from Figure 7 that for acyclic directed graphs there is no error edge when the magnetic force is strong.

3.1.3 Cyclic directed graphs

What is most interesting in drawing cyclic directed graphs in a parallel field is whether the number of "feedback" edges is close to minimal or not. Figure 9 displays a good example from our algorithm. In Figure 9f only one edge ($0 \rightarrow 4$) is pointing upward whereas all other edges downward. This means that the minimum feedback edge set problem is solved. Of course, this can not be confirmed by statistical experiments in general. However, the number of feedback edges (or error edges) is low (about 10% of $|E|$) in the strength of the parallel field as seen in Figure 7.

3.2 Results in orthogonal field

3.2.1 Edge-bipartite rooted trees

Figure 10 shows variations of layouts of an edge-bipartite rooted tree that represent h-v drawings[8] of a list structure (see Figure 2a). An edge-bipartite rooted tree is placed in an orthogonal field and its layouts are calculated changing the strength of the field. Though there is no crossing in Figure 10, we can not always eliminate crossings even if we use the two-phase algorithm. Figure 11 shows several examples of layouts of larger rooted trees where the orientations of edges conform well to the field but there remain several crossings. Results of statistical experiments are shown in Figure 12 in each case.

3.2.2 Acyclic mixed graphs

The directed graph presented in Figure 2b is drawn by our magnetic-spring algorithm where three isolated vertices are omitted. Though directed edges of the graph usually are replaced with one-directional magnetic springs, both-way relationships (↔) are replaced with bi-directional magnetic springs in this case. It is aimed that the former is laid out upward and the latter horizontally in the orthogonal field. Figure 13 shows variations of layouts of the graph calculated in different strengths of the field.

In the acyclic mixed graph presented in Figure 2c, one-directional relationships are replaced with one-directional magnetic springs and three types of bi-directional relationships all are replaced with bi-directional magnetic springs. Then our algorithm is applied to the graph so that the former relationships are drawn downward and the latter horizontally as much as possible. Figure 14 shows variations of diagrams of the acyclic mixed graph where we can distinguish one-directional relationships from bi-directional relationships more easily in the case of the strong field than in the case of no field. Results of statistical experiments are shown in Figure 12.

3.3 Results in polar field

Reggiani and Marchetti(1988)[12] founded that if a vertex-bipartite graph was drawn as a hierarchy with two horizontal levels then its diagram could not avoid many crossings (see Figure 15a), whereas if it was drawn as a hierarchy with two concentric discs then its diagram could avoid crossings completely (see Figure 15b). In order to check this ability of our algorithm, we place the same graph in the polar field and apply our algorithm to it where an anchor vertex connecting to vertices with numeric labels is placed at the origin, but the anchor is not displayed. Figure 15c is a resulted diagram where the orientation of every edge conforms to the orientation of the field, but three crossings can not be eliminated. Cases for no field and a parallel field also are displayed in Figures 15d and 15e respectively. In Figure 15d the number of crossings is very low, but orientations of edges have no regularity. In Figure 15e the downward drawing is attained, but several crossings remain.

3.4 Results in concentric field

Figure 16 shows variations of layouts of a cyclic directed graph (tetragonal and pentagonal pillars) obtained from our algorithm when the strength of a concentric field is changed. Figures 16a and 16d correspond to the cases of no field and Figures 16c and 16f the strongest. When we increase the field strength, we can obtain symmetrical layouts where the conformity to the orientation of the field is attained, which bring us the easiness for grasping cycles. We check whether this advantage of our algorithm arises even for more general cases. Figure 17 shows variations of layouts of a more general cyclic directed graph (same graph as Figure 9) where we can recognize cycles easily when the field becomes strong. Results of statistical experiments are shown in Figure 18.

4. Concluding remarks

We have proposed a novel method for drawing graphs based upon magnetic-spring model that is an extension of Eades's spring model. Graph drawing by force-directed placement so far has been investigated mainly for drawing undirected graphs and has not considered a control of edge orientations. Our method realizes to control edge orientations and therefore can enlarge classes of diagramming objects into not only undirected graphs but also trees, directed graphs and mixed graphs. This means that with the magnetic-spring algorithm we can draw extensive classes of graphs nicely in a simple and unified manner. Moreover, since this method is conceptually intuitive, it is quite easy to understand, implement and improve the method, and adjust parameters.

To define the magnetic-spring model we have newly introduced magnetic-springs, magnetic fields and magnetic forces imitating physical systems, but they all are "virtual" or do not have to reflect the natural reality accurately. Two types of magnetic springs (one-directional and bi-directional) and several types of magnetic fields (parallel, polar, concentric, orthogonal and polar-concentric) have been considered.

We have demonstrated the performance of our method showing a lot of layout examples and making statistical experiments. In investigating the performance, our interests has existed in the following problems:

(1) Can rooted trees be drawn without crossings or with few crossings? (See subsection 3.1.1.)

(2) Can Downward (or upward) drawing of acyclic directed graphs be easily realized? (See subsection 3.1.2.)

(3) How about relationships between our method and the feedback edge set problem in the case of drawing cyclic directed graphs? (See subsection 3.1.3.)

(4) Is our method effective for h-v drawing[8] of rooted binary trees? (See subsection 3.2.1.)

(5) Can acyclic mixed graphs be drawn in a way that we can easily grasp a global structure constituted with different kinds of edges and distinguish them readily?

(6) To which kind of problems is a polar field applicable? (See subsection 3.3.)

(7) Can cyclic directed graphs be drawn in a way that it is easy to grasp the global flow of the graphs and the existence of cycles? (See subsection 3.4.)

Since the magnetic-spring method is substantially heuristic, we have not been able to give exact answers to the above-stated problems. However, the results of preliminary experiments presented in section 3 tell us extensive effectiveness of the magnetic-spring method, especially in problems (1), (2), (4), (5) and (7).

For future research it is envisaged to analyze more precisely trade-off relationships among aesthetic criteria, to diversify the idea of "field", to extend "virtual" models and to sophisticate formulations and algorithms in both theoretical and practical senses.

References

1. P. Eades and R. Tamassia (1989) Algorithms for drawing graphs: An annotated bibliography, Tech. Rep. CS-89-09, Dept. of Computer Science, Brown Univ.
2. P. Eades (1984) A heuristic for graph drawing, *Congressus Numerantium* **42**, 149-160.
3. T. Fruchterman and E. Reingold (1991) Graph drawing by force-directed placement, *Software - Practice and Experience* **21**-11, 1129-1164.
4. T. Kamada, T. (1988) On visualization of abstract objects and relations, Dr. S. thesis, Univ. of Tokyo.
5. C. Batini, M. Talamo and R. Tamassia (1982) Computer aided layout of Entity-Relationship diagrams, *J. Systems and software* **4**, 163-173.
6. G. Kant, G. (1993) Algorithms for drawing planar graphs, Ph. D. thesis, Univ. of Utrecht.
7. R. Tamassia, R. Di Battista and C. Batini (1988) Automatic graph drawing and readability of diagrams, *IEEE Trans. Systems, Man, and Cybernetics* **SMC-18**-1, 61-79.
8. T. Lin (1993) A general schema for diagrammatic user interfaces, Ph. D. thesis, Univ. of Newcastle.
9. D. W. Malone (1975) An introduction to the application of interpretive structural modeling, *Proc. IEEE* 63-3, 397-404.
10. M. J. Bickerton (1992) A practitioner's handbook of requirement engineering methods and tools, Oxford Univ.
11. P. Eades (1991) Drawing free trees, Res. Rep. IIAS-RR-91-17E, Intern. Inst. for Advanced Study of Social Information Science, Fujitsu Lab. Ltd., 29pp.
12. M. G. Reggiani and F. E. Marchetti (1988) A proposed method for representing hierarchies, *IEEE Trans. Systems, Man, and Cybernetics* SMC-**18**-1, 2-8.

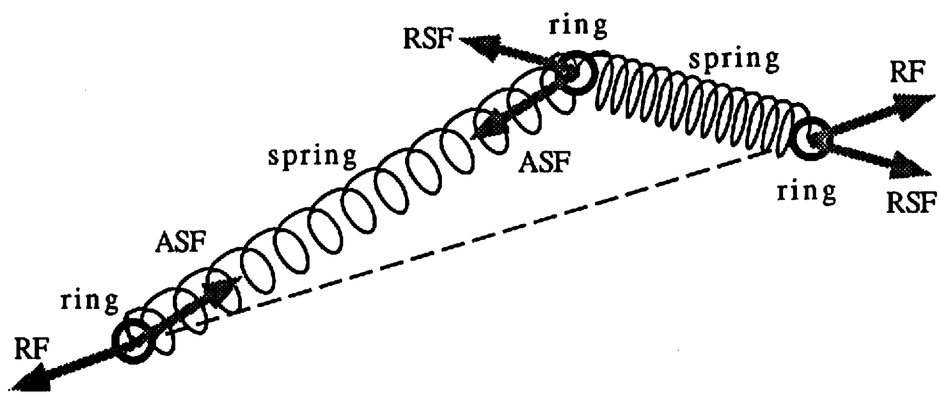

(a)

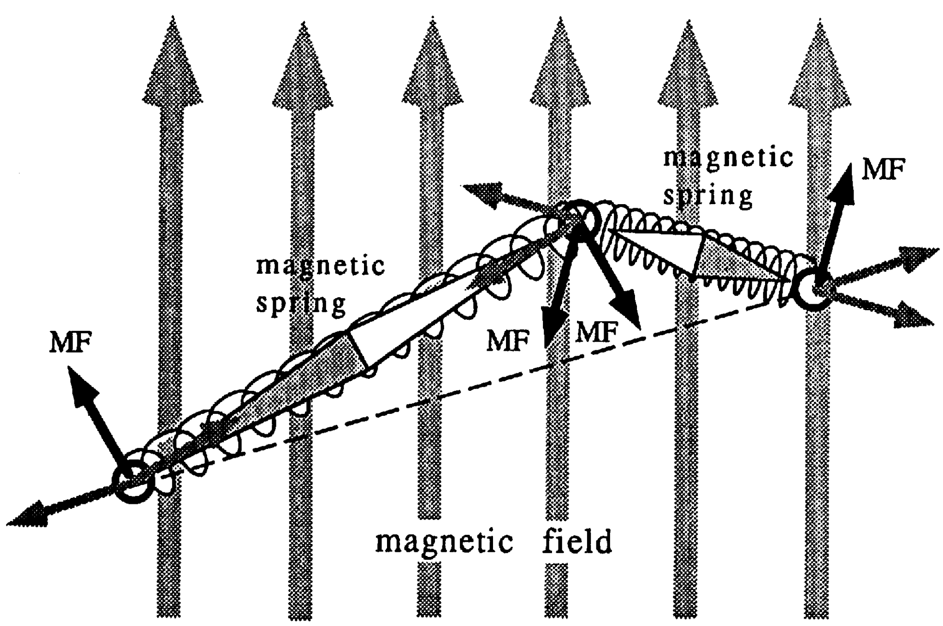

(b)

Figure 1. Spring model(a) and magnetic-spring model(b).
ASF: attractive spring force, RSF: repulsive spring force,
RF: repulsive force and MF: magnetic force.

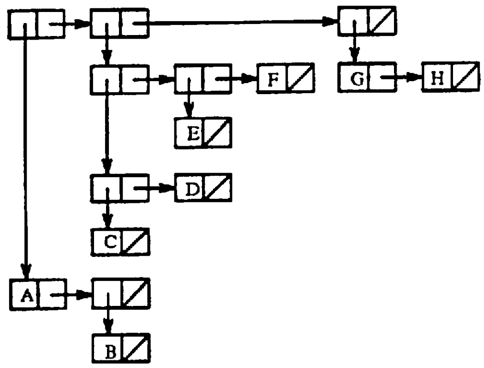

Figure 2a. A list structure diagram [8].

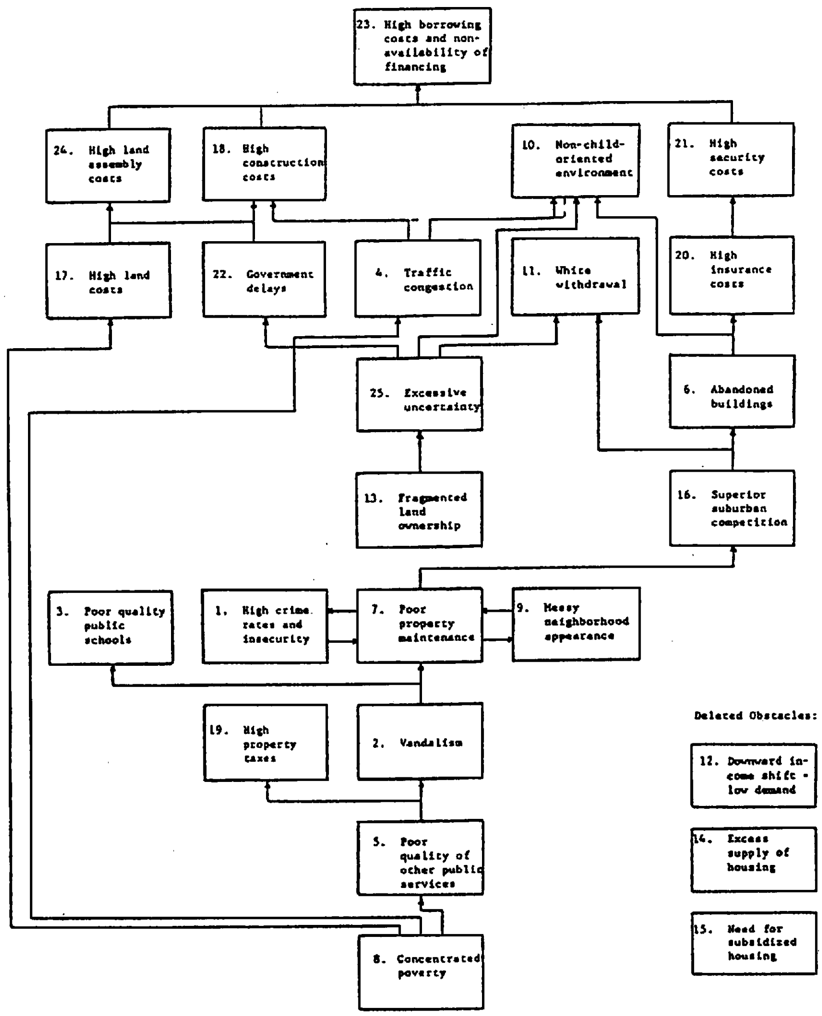

Figure 2b. A causal relationship diagram [9].

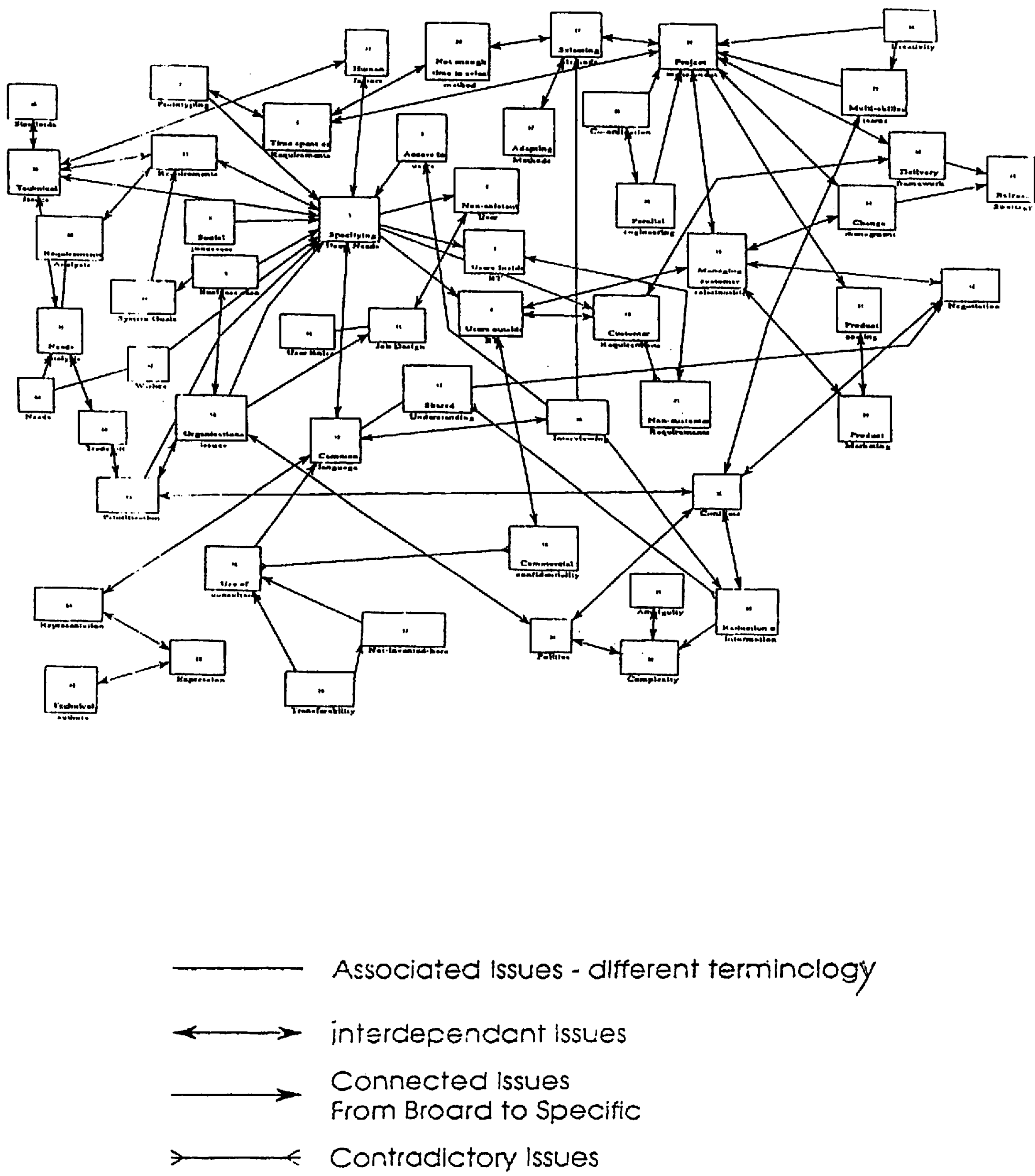

Figure 2c. An issue map [10].

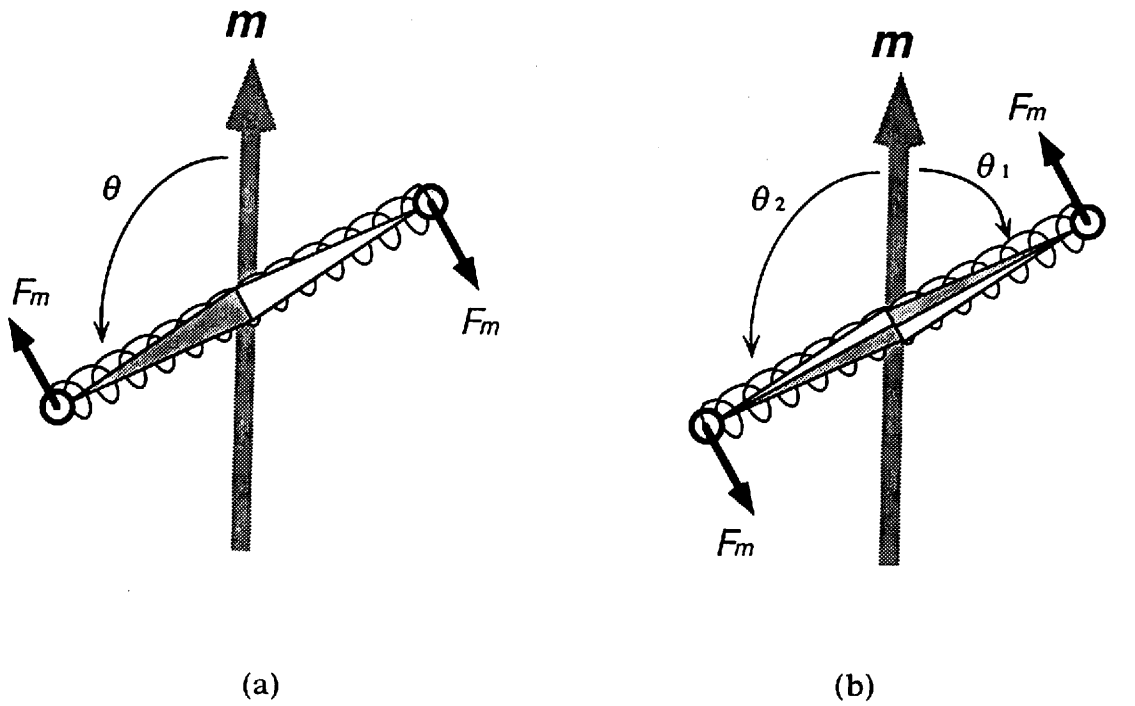

Figure 3. One-directional springs (a) and bi-directional springs (b), and magnetic forces.

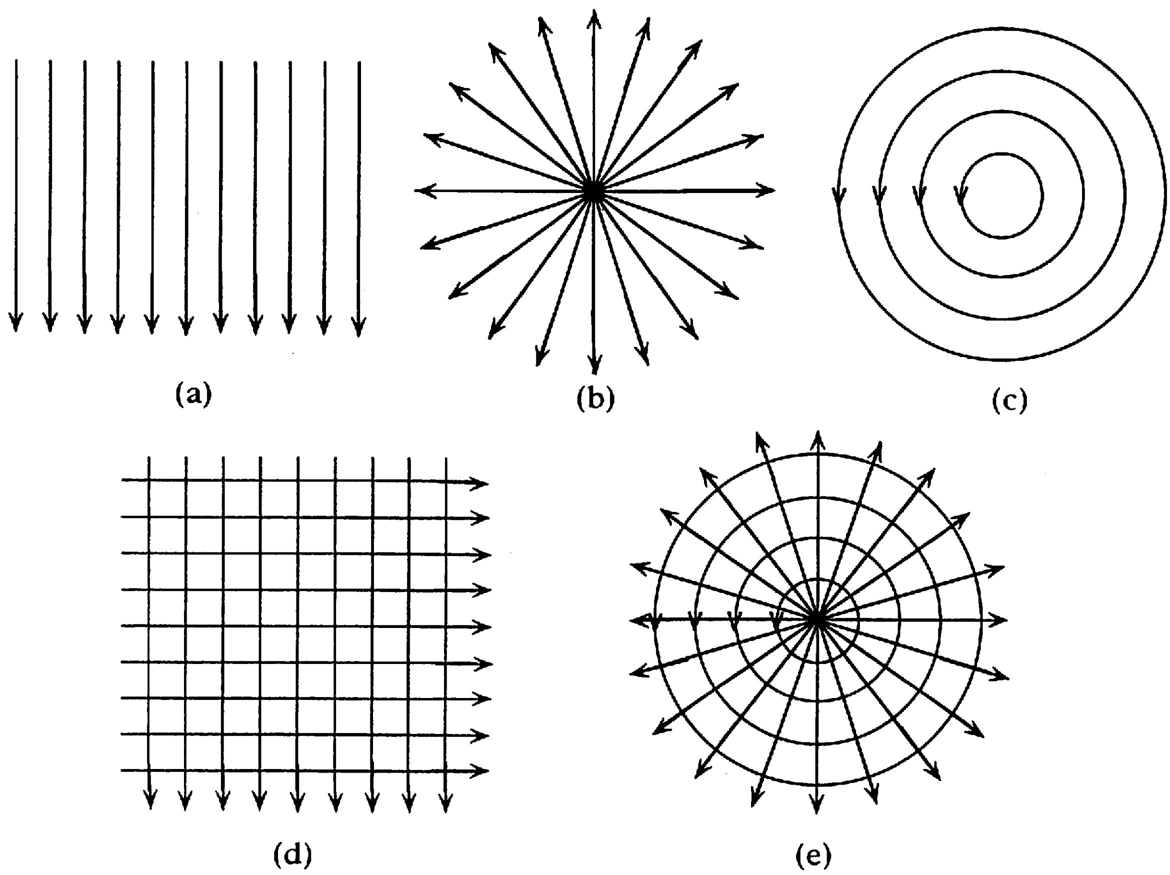

Figure 4. Standard and compound mangetic fields:
(a) parallel(south), (b) polar, (c) concentric (anti-clockwise),
(d) orthogonal and (e) polar-concentric.

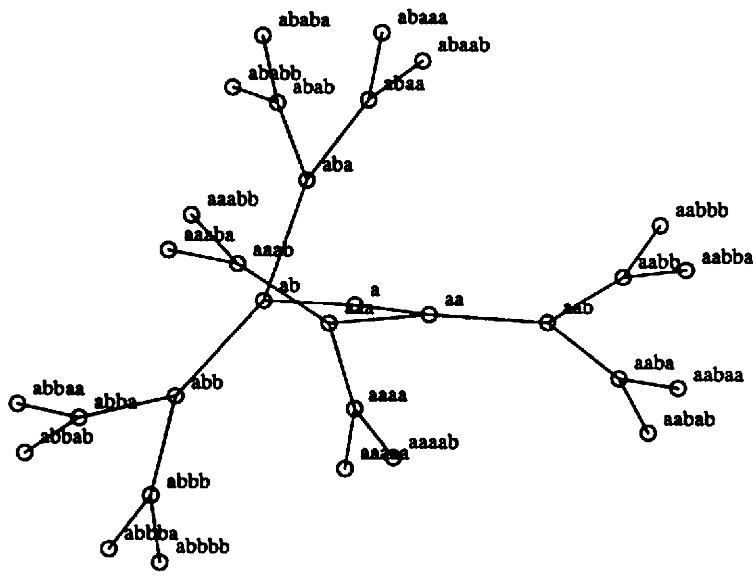

Figure 5. Example of a potential barrier in drawing trees [3].

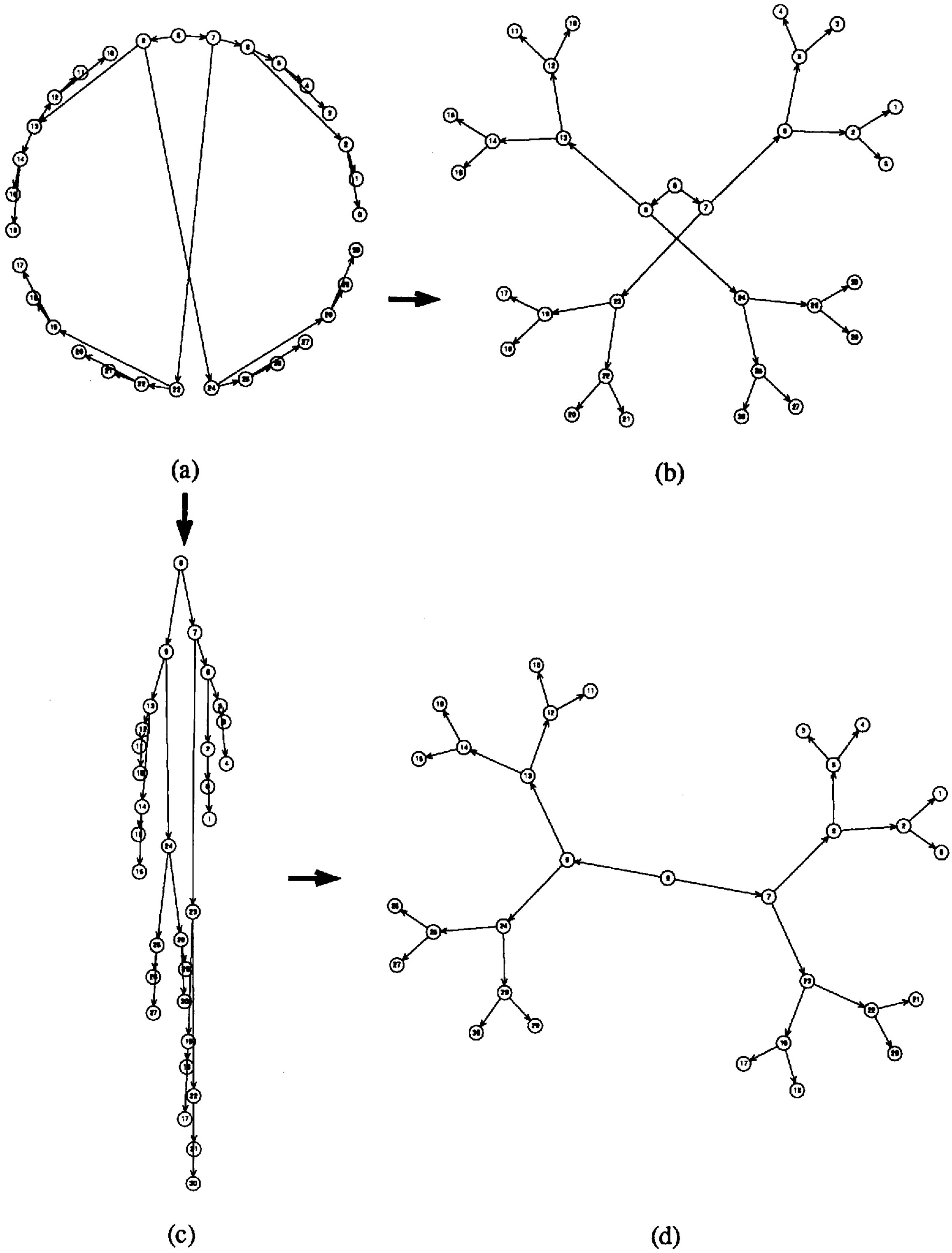

Figure 6. A good result from magnetic-spring algorithm.
(a) initial placement, (b) layout in no field, (c) layout in the strong field and
(d) layout after two phases.

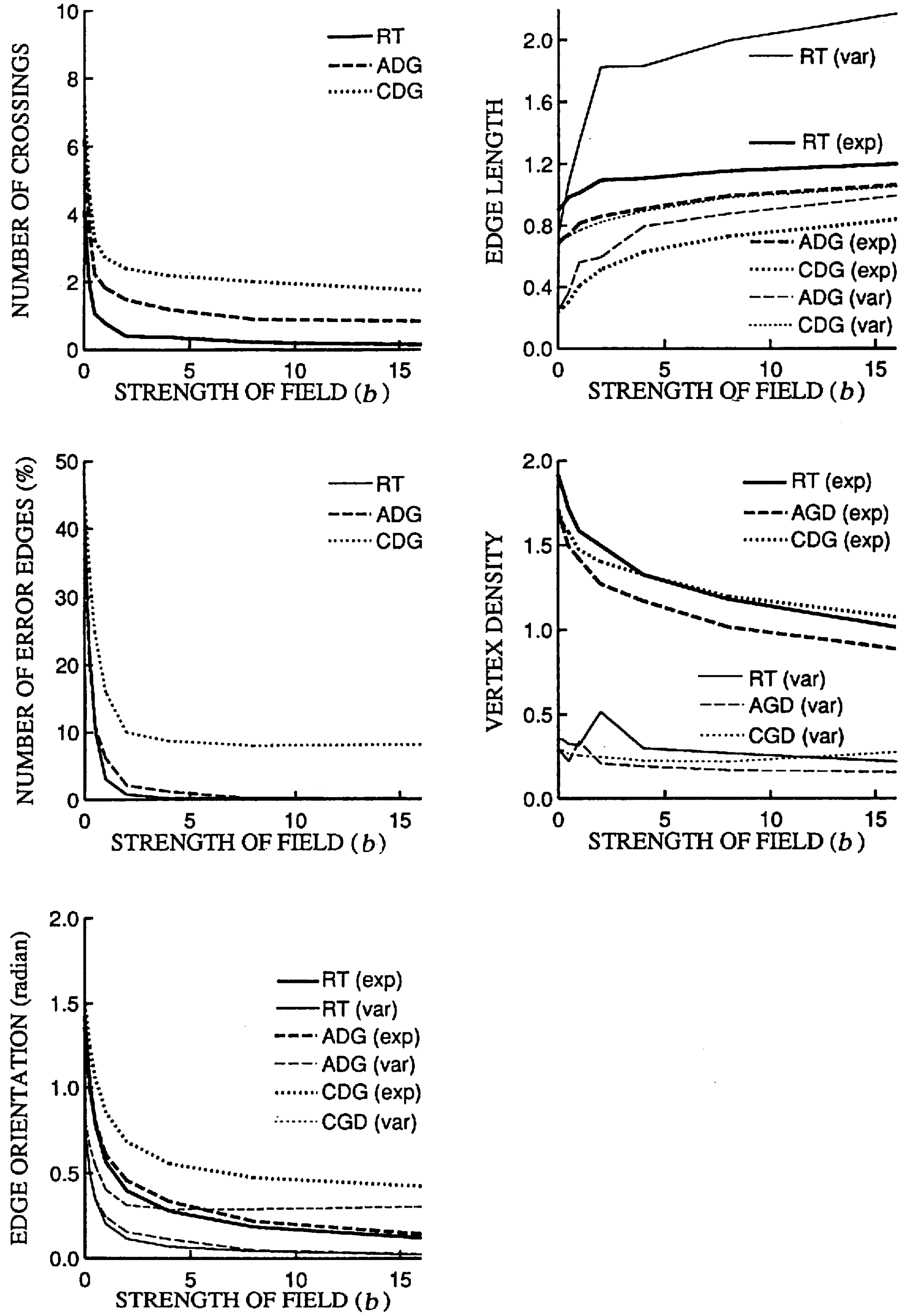

Figure 7. Results of statistical experiments in the parallel field.
RT(vertices: 40), ADG(vertices: 20), CDG(vertices: 20)

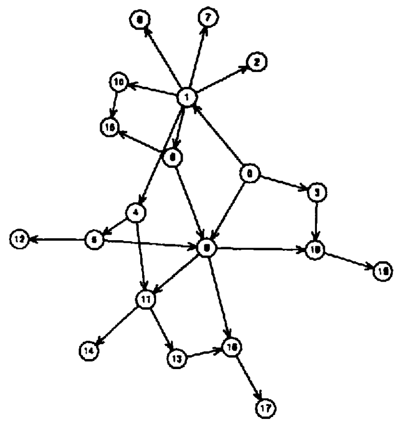

(a) $b = 0$

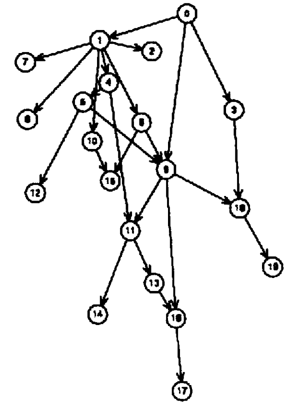

(b) $b = 1$

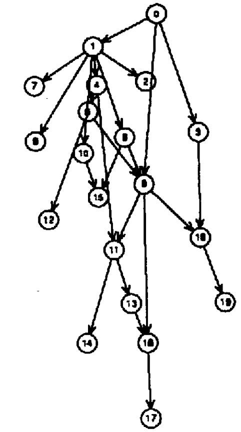

(c) $b = 2$

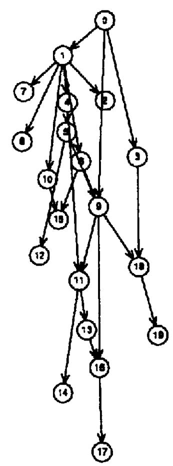

(d) $b = 4$

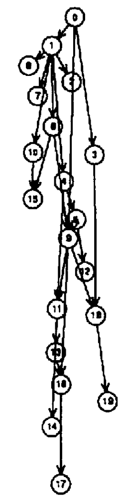

(e) $b = 8$

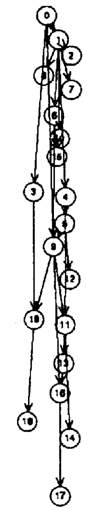

(f) $b = 16$

Figure 8. Variations of layouts of an acyclic directed graph (vertices: 20) in different strengths of the parallel field.

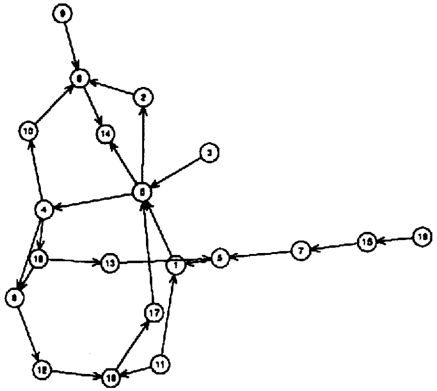

(a) $b = 0$

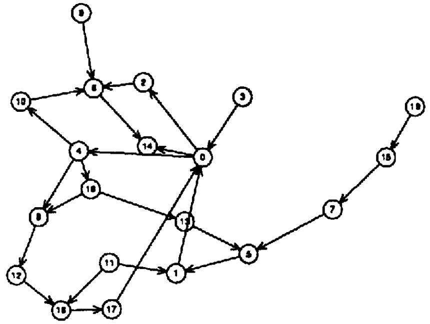

(b) $b = 0.5$

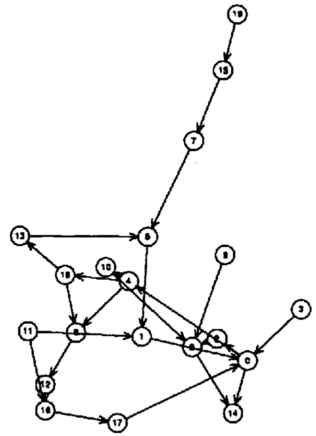

(c) $b = 1$

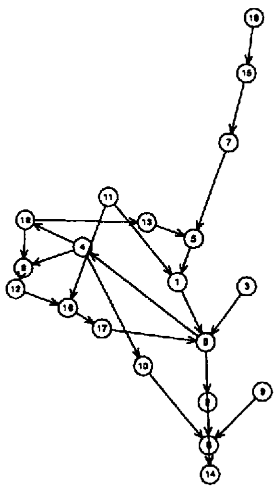

(d) $b = 2$

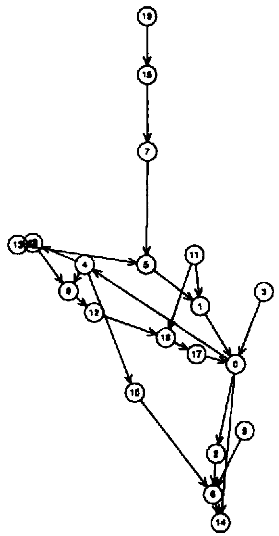

(e) $b = 4$

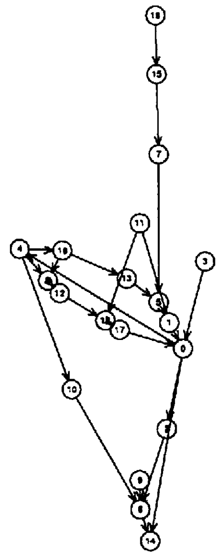

(f) $b = 8$

Figure 9. Variations of layouts of a cyclic directed graph (vertices: 20) in different strengths of the parallel field.

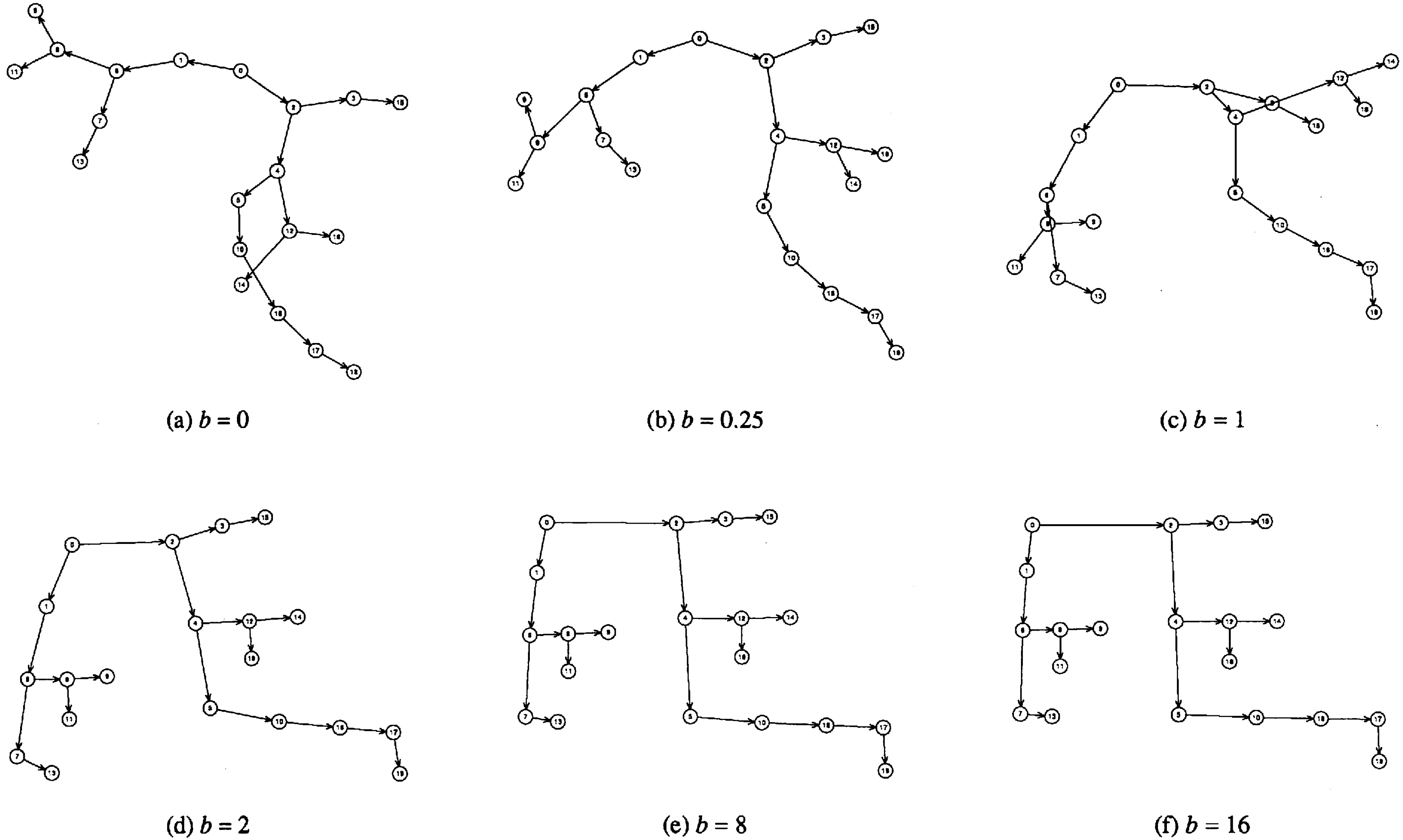

Figure 10. Variations of layouts of an edge-bipartite rooted tree (vertices: 20) in different strengths of the orthogonal field.

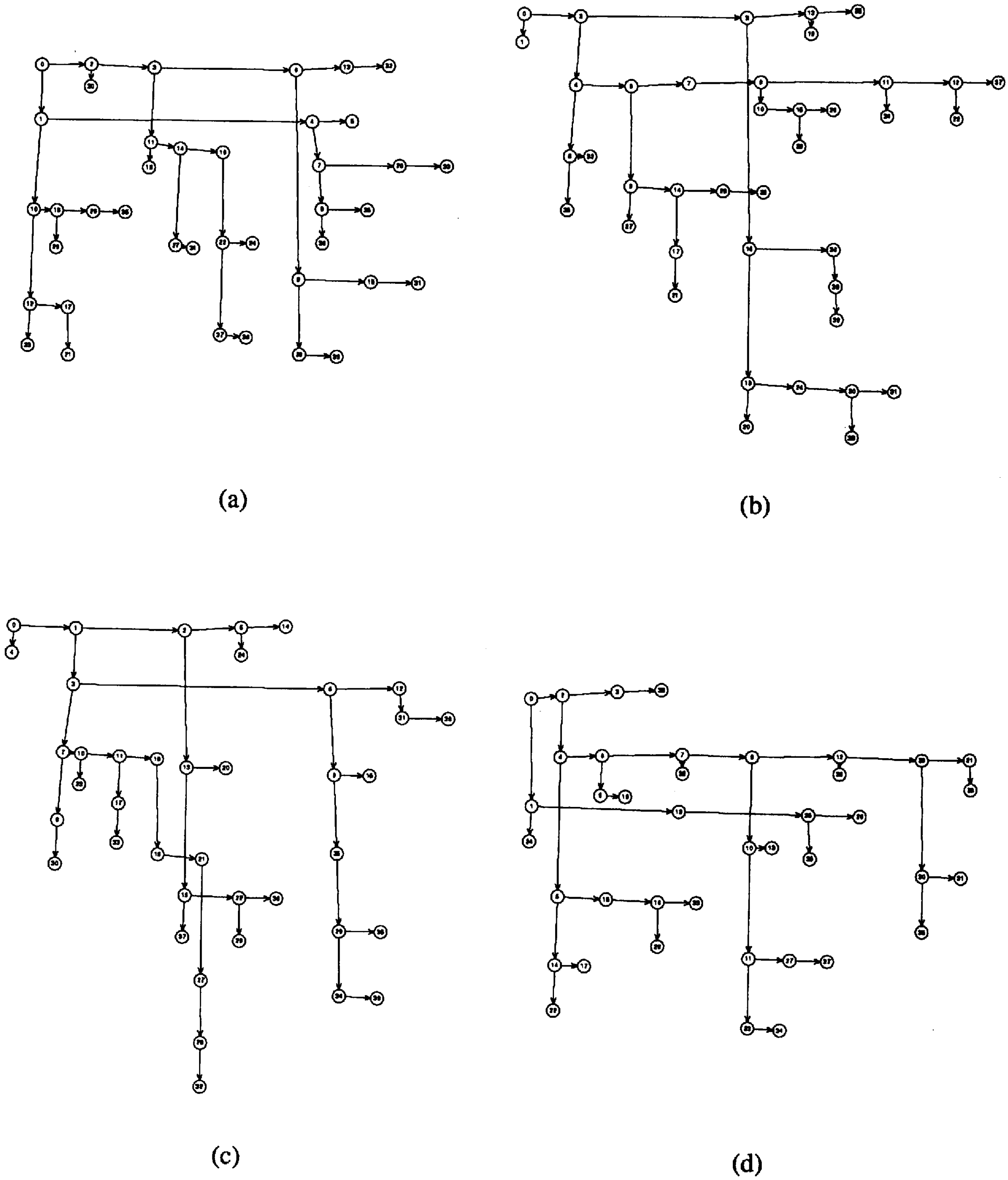

Figure 11. Examples of layouts of larger edge-bipartite rooted trees (vertices: 40) in the orthogonal field.

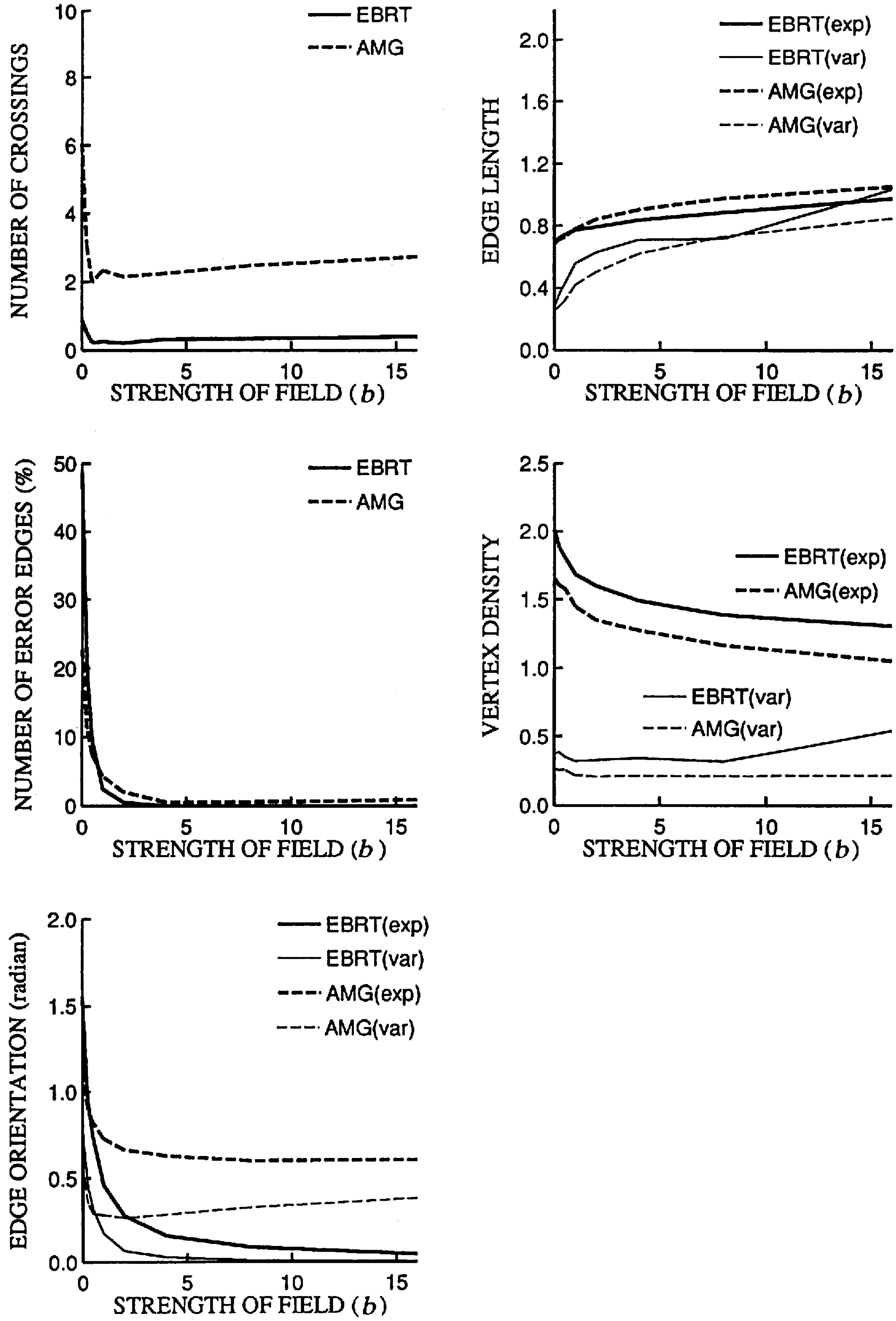

Figure 12. Results of statistical experiments in the orthogonal field.
EBRT(vertices: 20), AMG(vertices: 20)

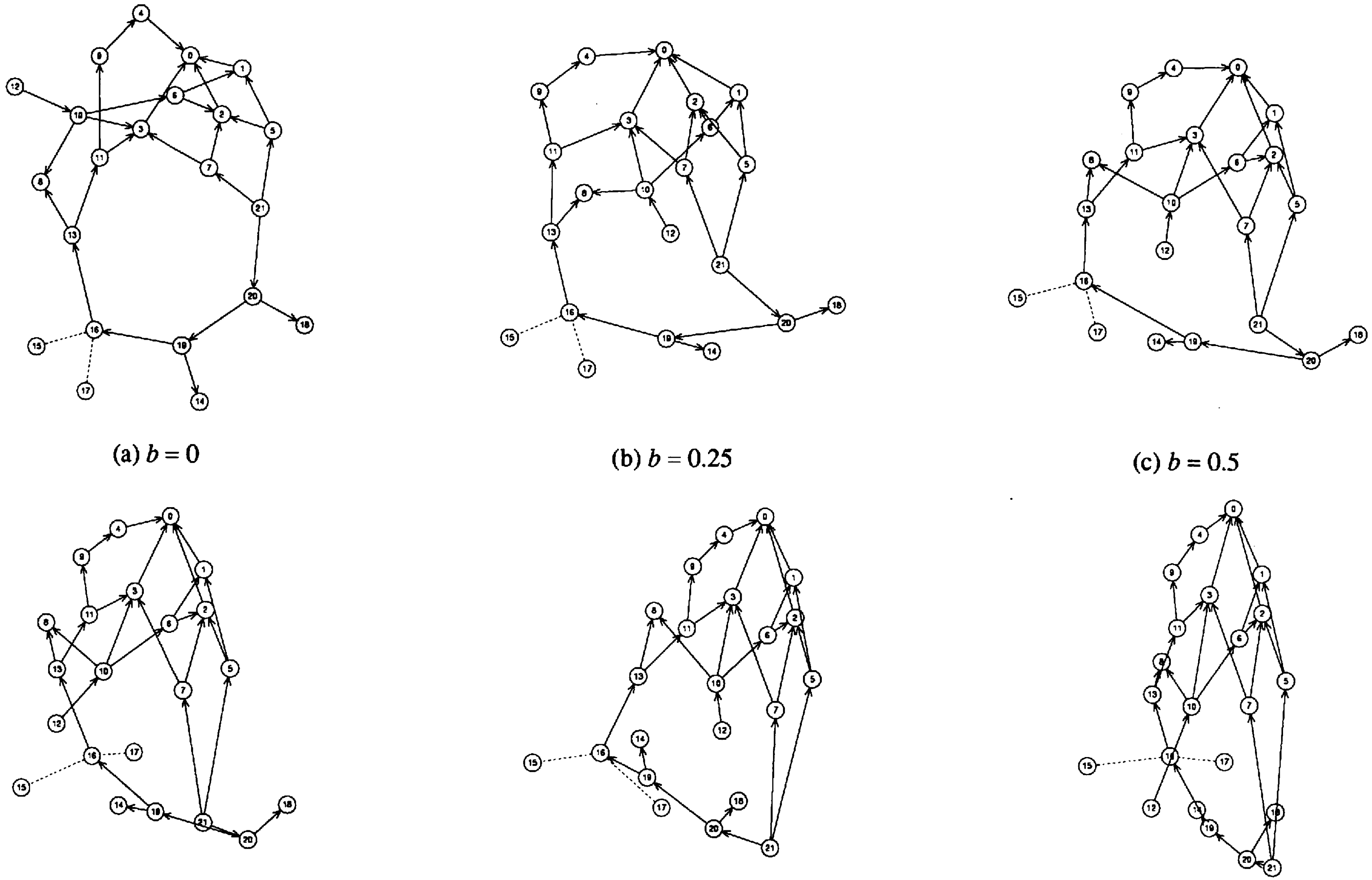

(a) $b = 0$ (b) $b = 0.25$ (c) $b = 0.5$

(d) $b = 1$ (e) $b = 2$ (f) $b = 4$

Figure 13. Variations of a causal relationship diagram[9] in different strengths of the orthogonal field.

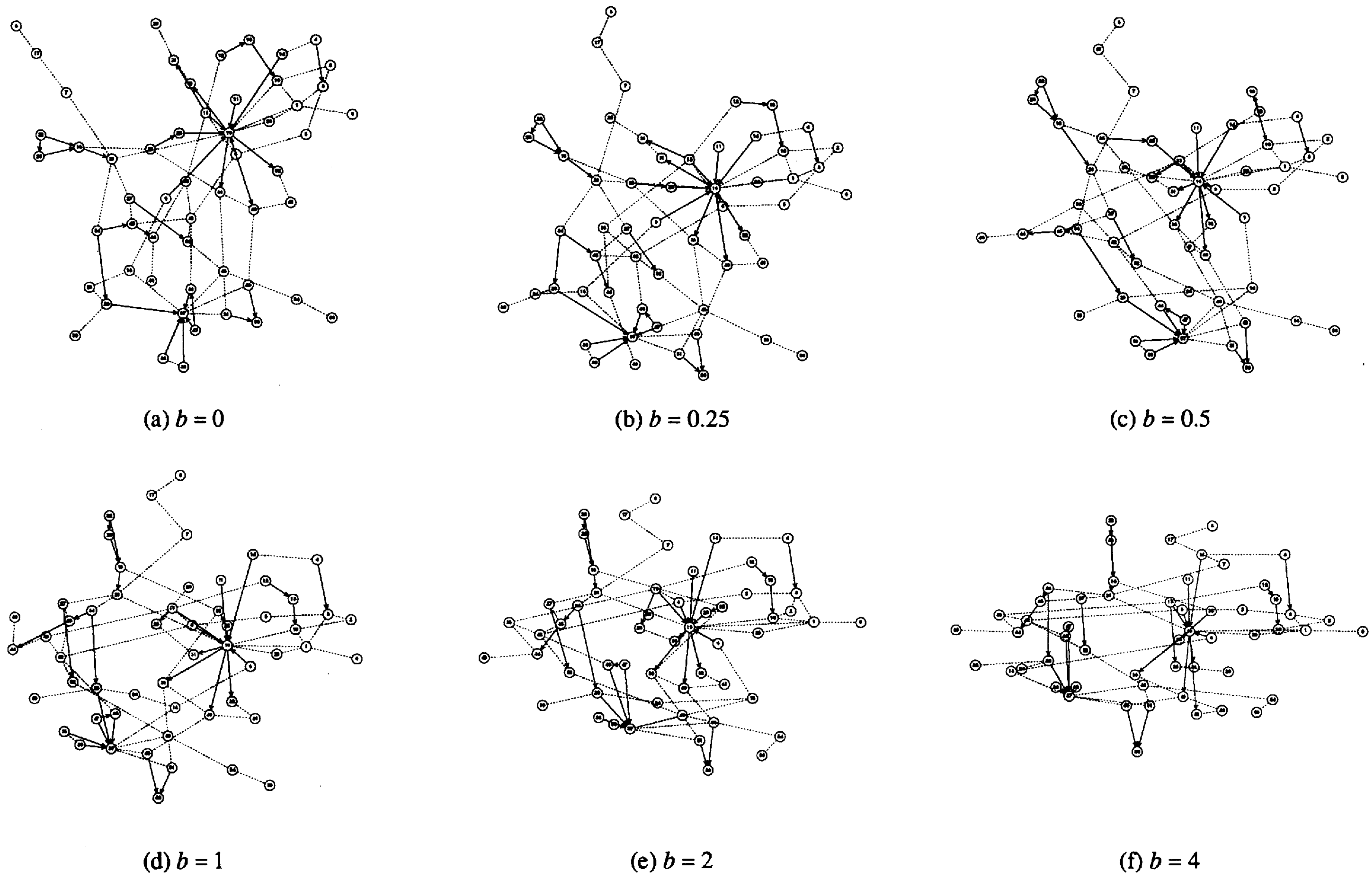

Figure 14. Variations of diagrams of an acyclic mixed graph[10] in different strengths of the orthogonal field.

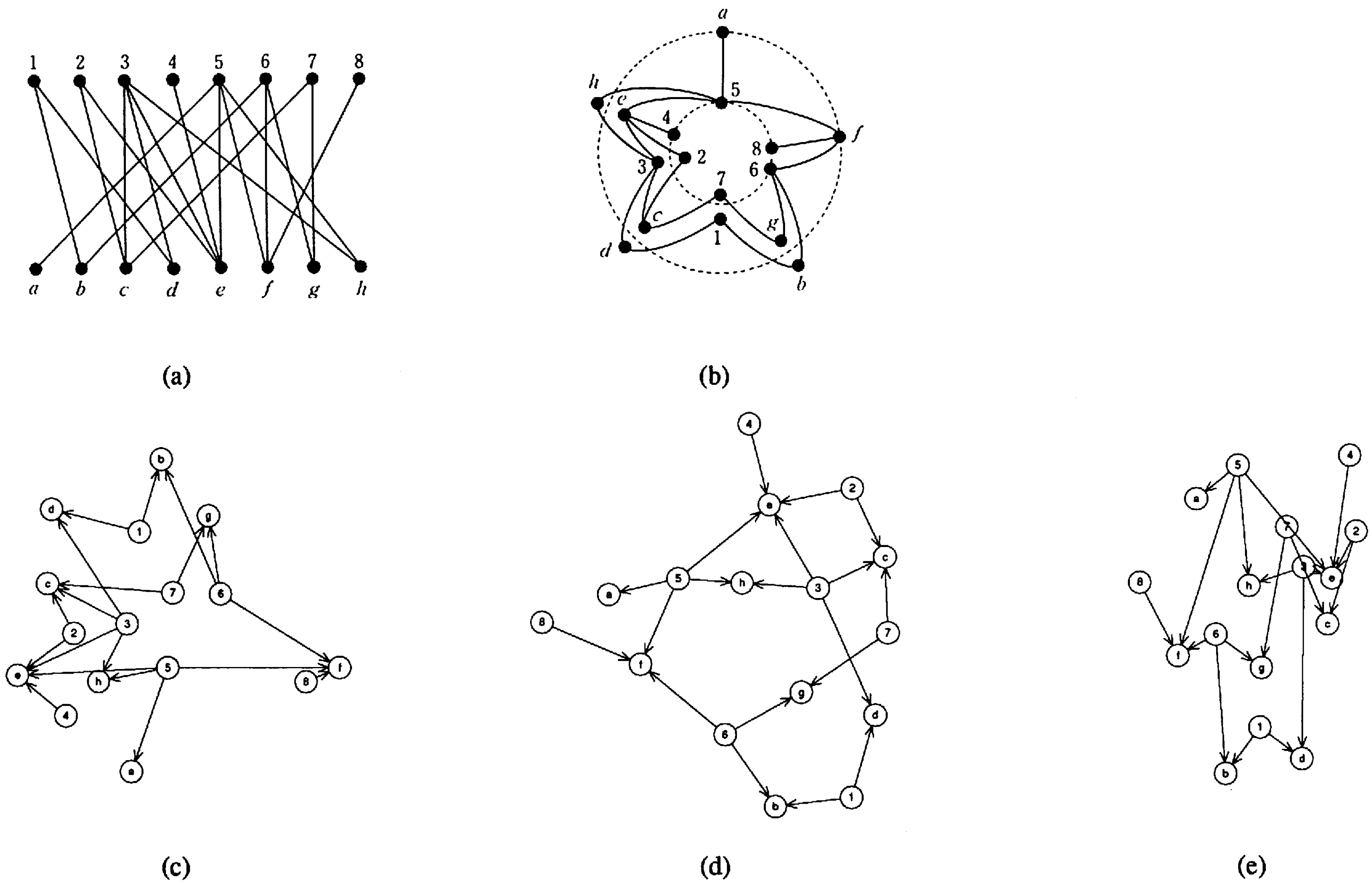

Figure 15. Comparisons among layouts of a vertex-bipartite graph by several drawing methods.

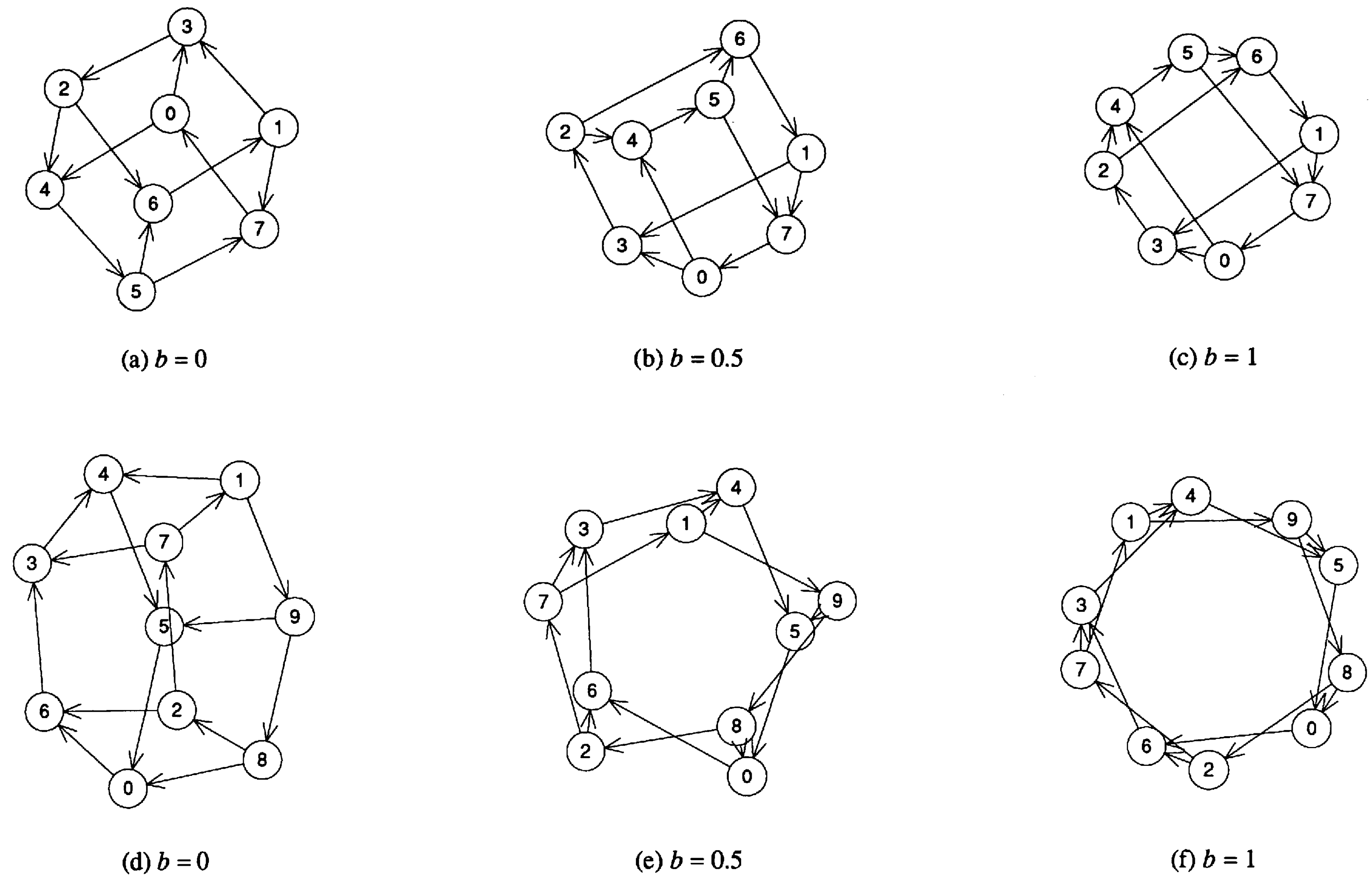

Figure 16. Variations of layouts of two cyclic directed graphs in different strengths of the concentric field.

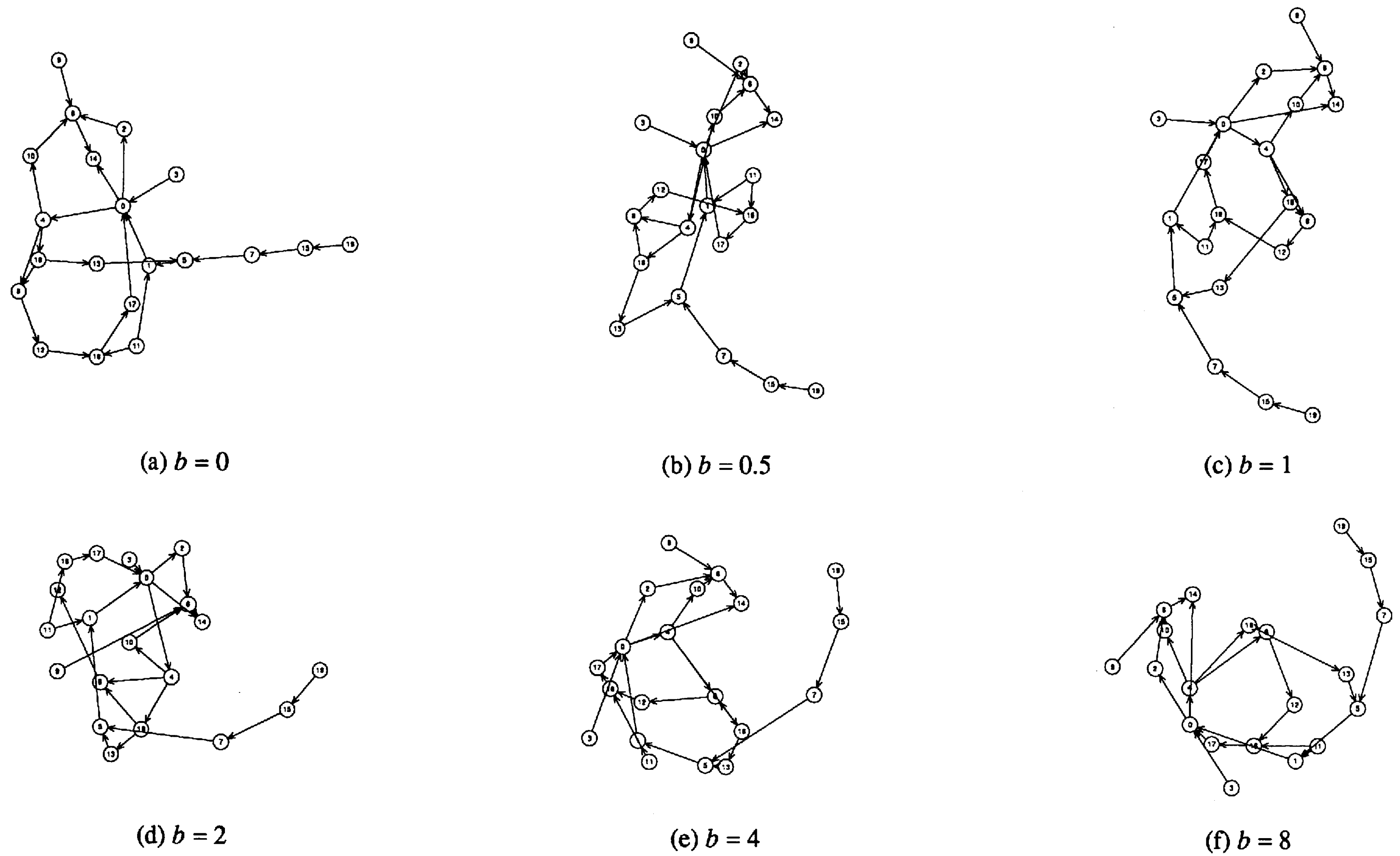

(a) $b = 0$ (b) $b = 0.5$ (c) $b = 1$

(d) $b = 2$ (e) $b = 4$ (f) $b = 8$

Figure 17. Variations of layouts of a more general cyclic directed graph (vertices: 20) in different strengths of the concentric field.

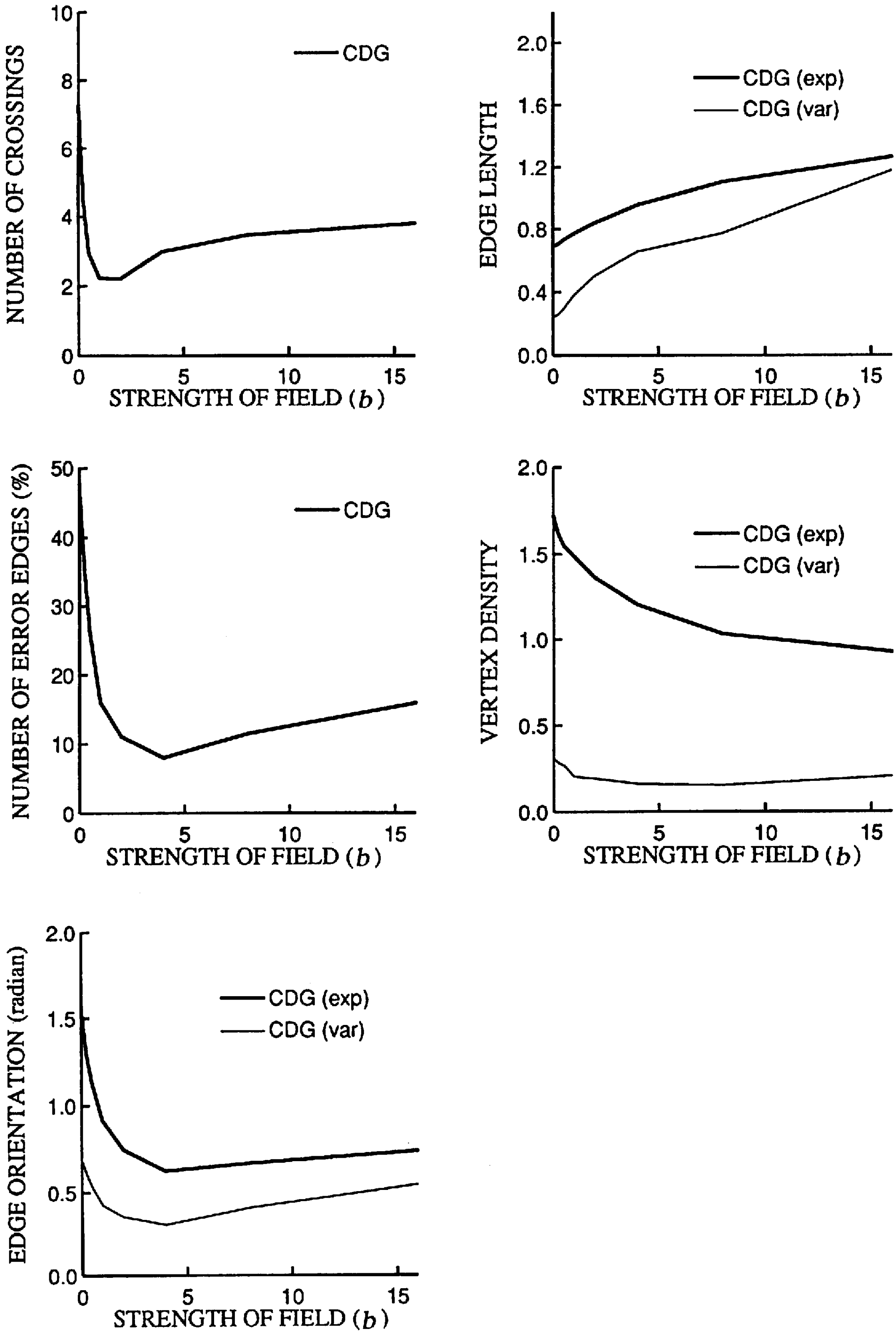

Figure 18. Results of statistical experiments in the concentric field.
CDG(vertices: 20)